

Synthesis of Pulse-Shaping Networks in the Time Domain

By DAVID A. SPAULDING

(Manuscript received February 11, 1969)

A fundamental problem in the design of data transmission systems is the synthesis of pulse-shaping networks which satisfy specifications in both the time and frequency domains. This paper considers the problem of designing a network to shape an arbitrary input pulse into a band-limited pulse having minimum intersymbol interference. The design procedure uses the zeros of the network transfer function to achieve the band-limiting properties (using a modified Temes and Gyi constraint) while the transfer function poles are optimized with a computer to give the desired time response.

By limiting the specifications on the shaped pulse to an absolute minimum, very accurate results are achieved with simple networks. Some sample designs and experimental results are included. For example, an 11th order transfer function is designed to shape rectangular pulses for a synchronous baseband pulse amplitude modulation system. The shaped pulses have a bandwidth 20 percent in excess of the Nyquist bandwidth and a theoretical worst-case distortion of 2.1 percent. An active realization of this transfer function achieved a worst-case distortion of about 2.5 percent.

I. INTRODUCTION

A fundamental problem in the design of data transmission systems is the synthesis of pulse-shaping networks which meet both time and frequency domain specifications. This paper considers the problem of designing, for a synchronous system, a network whose response to an arbitrary input pulse is a band-limited pulse with minimum intersymbol interference.¹ The design procedure uses a slightly modified Temes and Gyi procedure to keep the pulses band-limited;² the time response is optimized by using a computer. By focusing attention only on the important instants of time, very efficient and accurate designs result. We include some sample designs and experimental results.

II. PROBLEM DESCRIPTION

Consider a baseband pulse-amplitude modulation system in which information is coded as the amplitude values of a single pulse shape $x(t)$. Assume that a pulse is transmitted every T seconds over a channel, which for the present is ideal. The received signal, $s(t)$, is

$$s(t) = \sum_{n=-\infty}^{\infty} a_n x(t - nT),$$

where a_n is the amplitude of the n th pulse. The receiver samples $s(t)$ at T second intervals to determine the a_n . If one requires that the amplitude of any particular transmitted pulse can be determined by a single sample of the received signal, that is, for all integers m ,

$$s(mT + \tau) = \sum_{n=-\infty}^{\infty} a_n x(mT + \tau - nT) = a_m,$$

then $x(t)$ must be a pulse with zero intersymbol interference; that is,

$$x(nT + \tau) = \delta_{n0}, \quad (1)$$

where τ is some appropriate reference time and δ_{mn} is the Kroncker delta function.

Insofar as detecting the transmitted amplitude is concerned, no other specification on $x(t)$ is required. However, in most situations it is desirable, if not mandatory, to hand-limit the spectrum of $x(t)$ to frequencies less than some cutoff ω_c . Of course, the smallest allowable value for ω_c is π/T , the Nyquist frequency. Such a hand-limiting constraint might result from a requirement to limit adjacent channel interference. In many cases hand-limiting is the only frequency domain specification which is required. These simple time and frequency domain specifications represent the minimum requirements that a pulse-shaping network must meet in order to be useful in many pulse amplitude modulation systems (see Fig. 1). It is important to observe that such specifications do not uniquely define $x(t)$ except for the case where $\omega_c = \pi/T$.

Given these specifications, the problem now becomes that of generating a realizable rational transfer function which can achieve the specifications for a given input; that is, the approximation problem must be solved. With this problem solved, the physical network can be constructed using known techniques.

There are numerous ways of solving the approximation problem both in the time domain and the frequency domain. However, a more complete

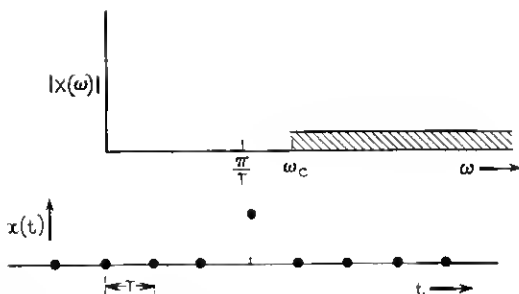


Fig. 1 — Minimum time and frequency domain specifications.

specification is generally required to use these techniques. For example, a standard frequency-domain approach is to completely specify a satisfactory $x(t)$ and to form the ideal transfer function of the network as $X(\omega)/Y(\omega)$, where $Y(\omega)$ is the Fourier transform of the network input. This transfer function is approximated by a rational function. The disadvantages of this straightforward approach are (i) whatever frequency domain measure of approximation accuracy is used, errors in the frequency domain are not easily related to errors at the sampling instants in the time domain, and (ii) completely specifying $x(t)$ requires the network to perform more shaping than is actually necessary. A particular selected $x(t)$ might give a transfer function which is more difficult to approximate than some other equally acceptable $x(t)$. Since the $x(t)$ most easily approximated is not known, specifying a particular $x(t)$ may require a transfer function of unnecessarily high order to achieve acceptable results.

Solving the approximation problem in the time domain permits more direct control of time domain errors. Ulstad has achieved good results in this manner; however, he completely specified $x(t)$.³ In general, time-domain approximation procedures provide no direct control of the band-limiting properties of the network and one must rely upon an accurate approximation of a completely specified $x(t)$ to achieve the band-limiting. Furthermore, when added weight in the approximation procedure is put at the sample times, the band-limiting properties of the network become increasingly difficult to control. This conflict, between approximating in the time domain with stress on sample times and achieving given band-limiting properties, seems to be common to most time-domain approximation techniques.

Jess and Schüssler considered the optimization of pulse-forming networks simultaneously in the time and frequency domains.⁴ Their

approach, although a step in the right direction, minimizes the tails of the pulse; this does not necessarily give an acceptable value of intersymbol interference when the rate at which pulses are transmitted is a significant percentage of the Nyquist rate for the bandwidth available.

What is required is a method of approximating in the time domain which constrains the frequency domain behavior to be band-limited. Temes and Gyi show how to develop transfer functions which have band-limited impulse responses.² These ideas can be applied, with some modification, to give a useful solution to the problem of pulse shaping.

III. PULSE SHAPING USING THE TEMES AND GYI CONSTRAINT

For convenience, Appendix A reviews the manner in which Temes and Gyi develop a low-pass transfer function which has an equal-ripple stopband behavior. This is accomplished by expressing the transfer function in partial fraction form and constraining the residues to depend on the poles in a particular manner. If $G(s)$ is a transfer function with one zero at infinity, it is expressed as

$$G(s) = \sum_{i=1}^N \frac{R_i}{s - s_i}, \quad (2a)$$

where

$$R_i = K z_i \prod_{\substack{j=1 \\ j \neq i}}^N \frac{z_i + z_j}{s_i - s_j} \quad (2b)$$

and $z_i^2 = s_i^2 + \omega_c^2$, $\text{Re } z_i \geq 0$; ω_c is the low-frequency edge of the stopband and K is the maximum gain in the stopband. It is important that this transfer function has all its zeros on the $j\omega$ axis and is therefore minimum phase.

In general, and specifically for the case where the input to the pulse-shaping network is a rectangular pulse, a minimum-phase transfer function does not have enough freedom to shape a pulse into a Nyquist pulse. (If a Nyquist pulse has a bandwidth of $(1 + \alpha)\pi/T$, where $0 < \alpha < 1$, then its Fourier transform must have linear phase over the frequency interval from zero to $(1 - \alpha)\pi/T$. To see this, compute the Fourier transform of the sampled pulse. This linear phase condition cannot be achieved, in general, with a minimum-phase shaping network.) To remedy this, the transfer function of equation (2) is multi-

plied by an all-pass transfer function which has the form,

$$H(s) = \prod_{i=N+1}^{N+L} \frac{-s - s_i}{s - s_i}; \quad \text{Re } s_i < 0. \quad (3)$$

The transfer function resulting from the product of equations (2) and (3) is band-limited and has arbitrary low-pass gain and phase characteristics. Observe that all the zeros of the transfer function $G(s)H(s)$ (half of the available degrees of freedom) are constrained to be functions of the poles in order to get the band-limiting behavior. The poles (the remaining degrees of freedom) can now be used to optimize the time behavior of the pulse.

Assume for the present that the pulse to be shaped is rectangular, that is,

$$y(t) = u(t) - u(t - T_o), \quad (4)$$

where $u(t)$ is the unit step function and T_o the pulse width. From equations (2), (3), and (4), the output pulse $x(t)$ is

$$x(t) = \sum_{i=1}^{N+L+1} \alpha_i \{u(t) \exp(s_i t) - u(t - T_o) \exp[s_i(t - T_o)]\}, \quad (5a)$$

where

$$\alpha_i = \begin{cases} \frac{R_i H(s_i)}{s_i}, & 1 \leq i \leq N \\ \frac{G(s_i)}{s_i} \prod_{j=N+1}^{N+L} \frac{-(s_i + s_j)}{(s_i - s_j)}, & N+1 \leq i \leq N+L \\ G(0), & i = N+L+1 \quad (s_{N+L+1} = 0) \end{cases} \quad (5b)$$

and only simple poles are assumed to occur.

Equation (5) gives the output pulse in terms of the network poles. The pulse can now be optimized in the time domain using a digital computer and an appropriate optimization technique. For the particular application considered here, only the values of $x(t)$ at equally spaced intervals of time are important, that is, $t = kT + t_o$, where k is a positive integer, T is the sampling interval, and $-T < t_o \leq 0$. By concentrating on these instants of time rather than on the entire pulse waveform, excellent pulse-shaping networks can be designed which are not excessively complex.

The pulse shaping networks given in the following examples were designed by using a general purpose optimization program written

by Mrs. J. M. Schilling. The program used a steepest descent minimization technique. Typical running times on an IBM 7094 were about three to four minutes.

Figures 2 through 12 show the results of two sample designs and some experimental measurements. The first example (Figs. 2 through 6) is a seventh-order network which shapes a rectangular pulse into a Nyquist pulse with 50 percent excess bandwidth.* The network stopband rejection is 40 dB and the output pulse has a worst-case distortion of 0.38 percent.† The second example (Figs. 7 through 12)

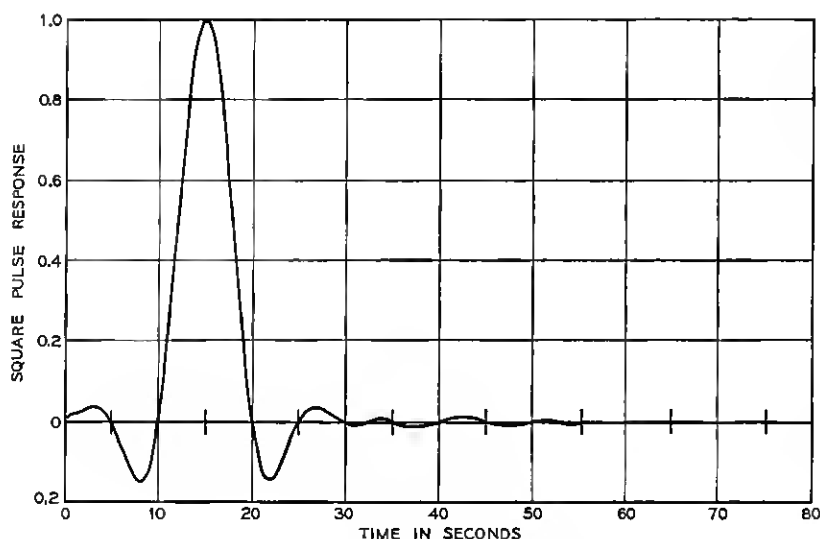


Fig. 2—Time response of a seventh order pulse-shaping network (one all-pass section) resulting from a rectangular input pulse of unit amplitude and of five seconds duration. The network has 40 dB stopband rejection, 50 percent excess bandwidth, and worst-case distortion of 0.38 percent. The Nyquist frequency is 0.1 Hz ($T = 5$ seconds).

shapes a rectangular pulse into a Nyquist pulse with 20 percent excess bandwidth. The worst-case distortion is 2.1 percent. For this example experimental measurements are shown for an active network realization using Tow's technique.⁵

* For a 50 percent excess bandwidth pulse, the low frequency edge of the stopband is at $(1.5/2T)$ Hz.

† Worst-case distortion is defined as $\sum_{k=-\infty}^{\infty} |x(kT + t_0)|$, where $x(k_0T + t_0) = 1$.

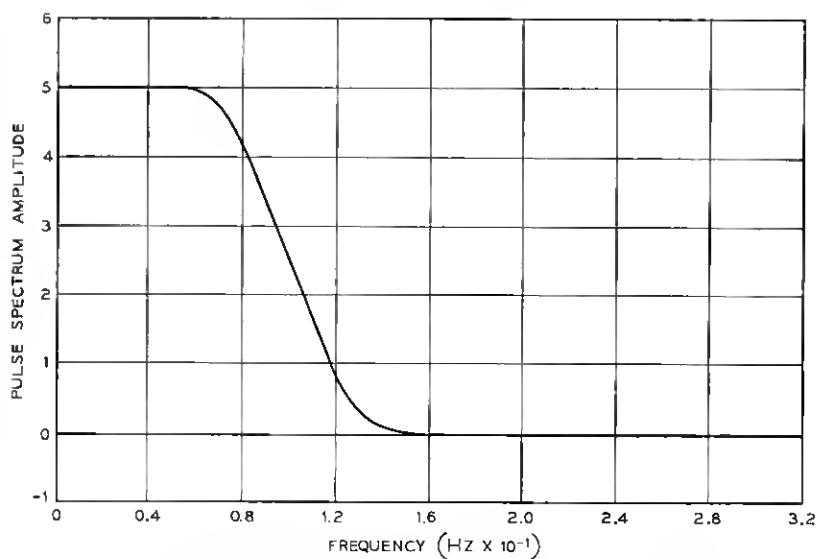


Fig. 3 — Pulse spectrum amplitude for time response shown in Fig. 2.

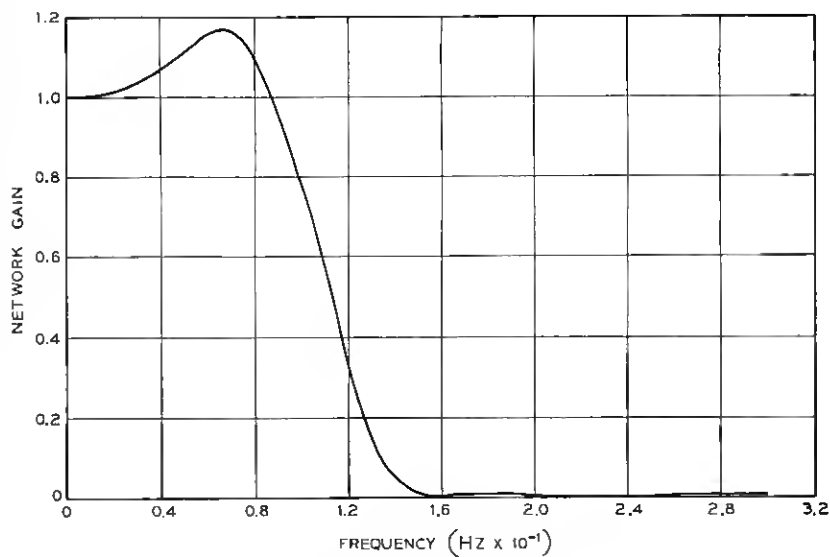


Fig. 4 — Gain of the network giving the output pulse shown in Fig. 2.

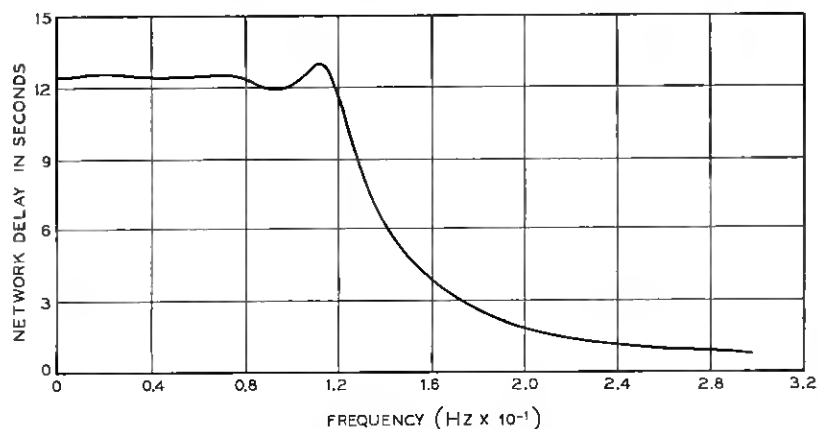


Fig. 5 — Delay of the network giving the output pulse shown in Fig. 2.

THE NUMERATOR POLYNOMIAL IS

$+ 3.996795\text{E-}02\text{S}^{**} 6$
 $+ -2.709413\text{E-}02\text{S}^{**} 5$
 $+ 1.275938\text{E-}01\text{S}^{**} 4$
 $+ -8.224750\text{E-}02\text{S}^{**} 3$
 $+ 9.840381\text{E-}02\text{S}^{**} 2$
 $+ -5.381433\text{E-}02\text{S}^{**} 1$
 $+ 1.244372\text{E-}02\text{S}^{**} 0$

THE DENOMINATOR POLYNOMIAL IS

$+ 1.000000\text{E+}00\text{S}^{**} 7$
 $+ 1.835959\text{E+}00\text{S}^{**} 6$
 $+ 2.200246\text{E+}00\text{S}^{**} 5$
 $+ 1.799349\text{E+}00\text{S}^{**} 4$
 $+ 1.018142\text{E+}00\text{S}^{**} 3$
 $+ 4.043381\text{E-}01\text{S}^{**} 2$
 $+ 1.012517\text{E-}01\text{S}^{**} 1$
 $+ 1.244925\text{E-}02\text{S}^{**} 0$

THE POLES ARE

$-1.999273\text{E-}01 \pm 4.918577\text{E-}01\text{J}$
 $-1.220059\text{E-}01 \pm 7.300850\text{E-}01\text{J}$
 $-3.389429\text{E-}01 \pm 2.046175\text{E-}01\text{J}$
 $-5.142068\text{E-}01 \quad 0. \quad \text{J}$

THE ZEROS ARE

$3.389439\text{E-}01 \pm 2.046168\text{E-}01\text{J}$
 $0. \quad \pm 9.768803\text{E-}01\text{J}$
 $0. \quad \pm 1.442686\text{E+}00\text{J}$

Fig. 6 — Transfer function data for the network of Figs. 2 through 5.

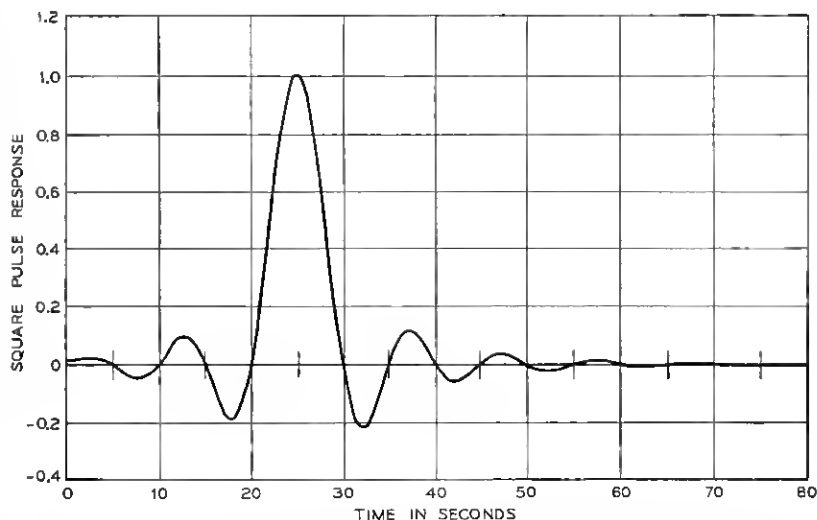


Fig. 7—Time response of an eleventh order pulse-shaping network (two all-pass sections) resulting from a rectangular input pulse of unit amplitude and of five seconds duration. The network has 35 dB stopband rejection, 20 percent excess bandwidth, and worst-case distortion of 2.1 percent. The Nyquist frequency is 0.1 Hz ($T = 5$ seconds). Note: 35 dB network stopband rejection gives 40 dB or better rejection of signal energy when a rectangular pulse of five seconds duration is the network input.

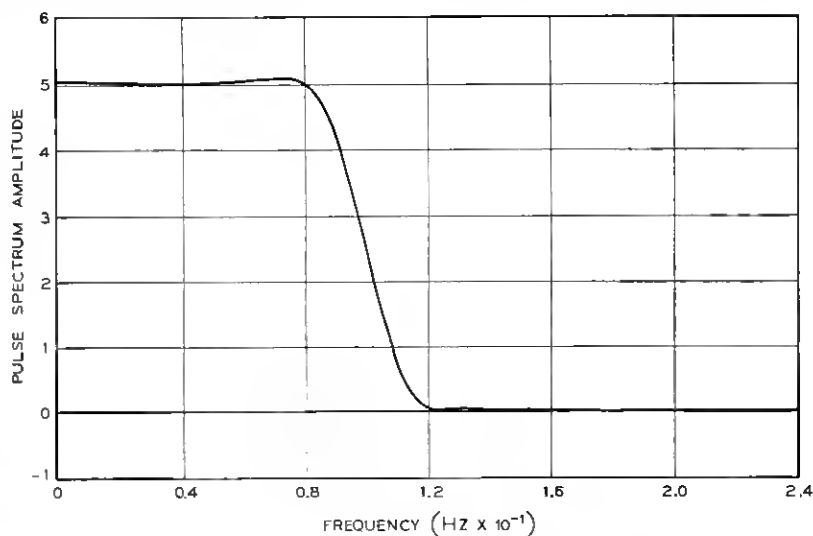


Fig. 8—Pulse spectrum amplitude for time response shown in Fig. 7.

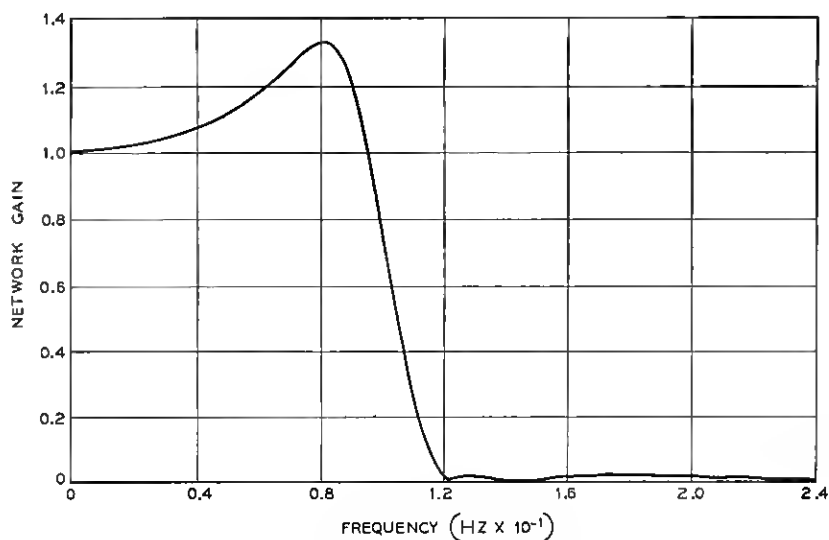


Fig. 9 — Gain of network giving the output pulse shown in Fig. 7.

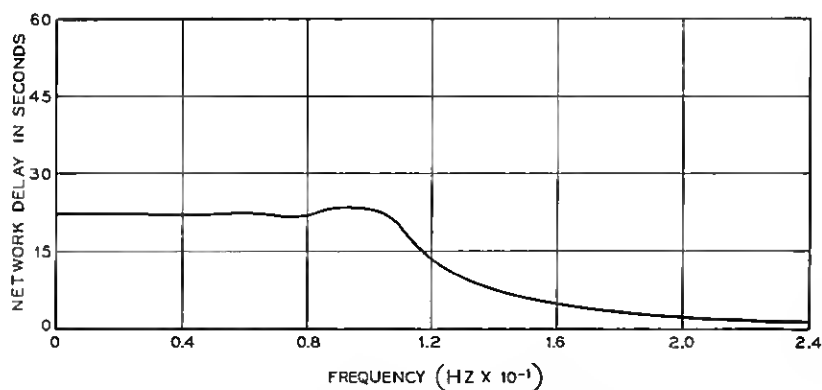


Fig. 10 — Delay of the network giving the output pulse shown in Fig. 7.

THE NUMERATOR POLYNOMIAL IS

$+ 9.010491E-02S^{**}10$
 $+ -7.116008E-02S^{**} 9$
 $+ 3.996278E-01S^{**} 8$
 $+ -2.963901E-01S^{**} 7$
 $+ 5.232092E-01S^{**} 6$
 $+ -3.347661E-01S^{**} 5$
 $+ 2.679873E-01S^{**} 4$
 $+ -1.276737E-01S^{**} 3$
 $+ 4.917976E-02S^{**} 2$
 $+ -1.105460E-02S^{**} 1$
 $+ 1.200169E-03S^{**} 0$

THE POLES ARE

$-4.895659E-01 \pm 4.424214E-01J$
 $-1.116714E-01 \pm 5.789655E-01J$
 $-8.819848E-02 \pm 6.881603E-01J$
 $-2.081902E-01 \pm 1.237181E-01J$
 $-1.866762E-01 \pm 3.768048E-01J$
 $-1.580778E+00 \quad 0. \quad J \quad 0.$

THE DENOMINATOR POLYNOMIAL IS

$+ 1.000000E+00S^{**}11$
 $+ 3.749382E+00S^{**}10$
 $+ 6.603178E+00S^{**} 9$
 $+ 8.185644E+00S^{**} 8$
 $+ 7.463441E+00S^{**} 7$
 $+ 5.326736E+00S^{**} 6$
 $+ 2.948257E+00S^{**} 5$
 $+ 1.289339E+00S^{**} 4$
 $+ 4.230783E-01S^{**} 3$
 $+ 1.019484E-01S^{**} 2$
 $+ 1.565021E-02S^{**} 1$
 $+ 1.194575E-03S^{**} 0$

THE ZEROS ARE

$1.866781E-01 \pm 3.768034E-01J$
 $2.081920E-01 \pm 1.237177E-01J$
 $0. \quad \pm 7.677332E-01J$
 $0. \quad \pm 9.111657E-01J$
 $0. \quad \pm 1.620049E+00J$

Fig. 11 — Transfer function data for the network of Figs. 7 through 10 and 12.

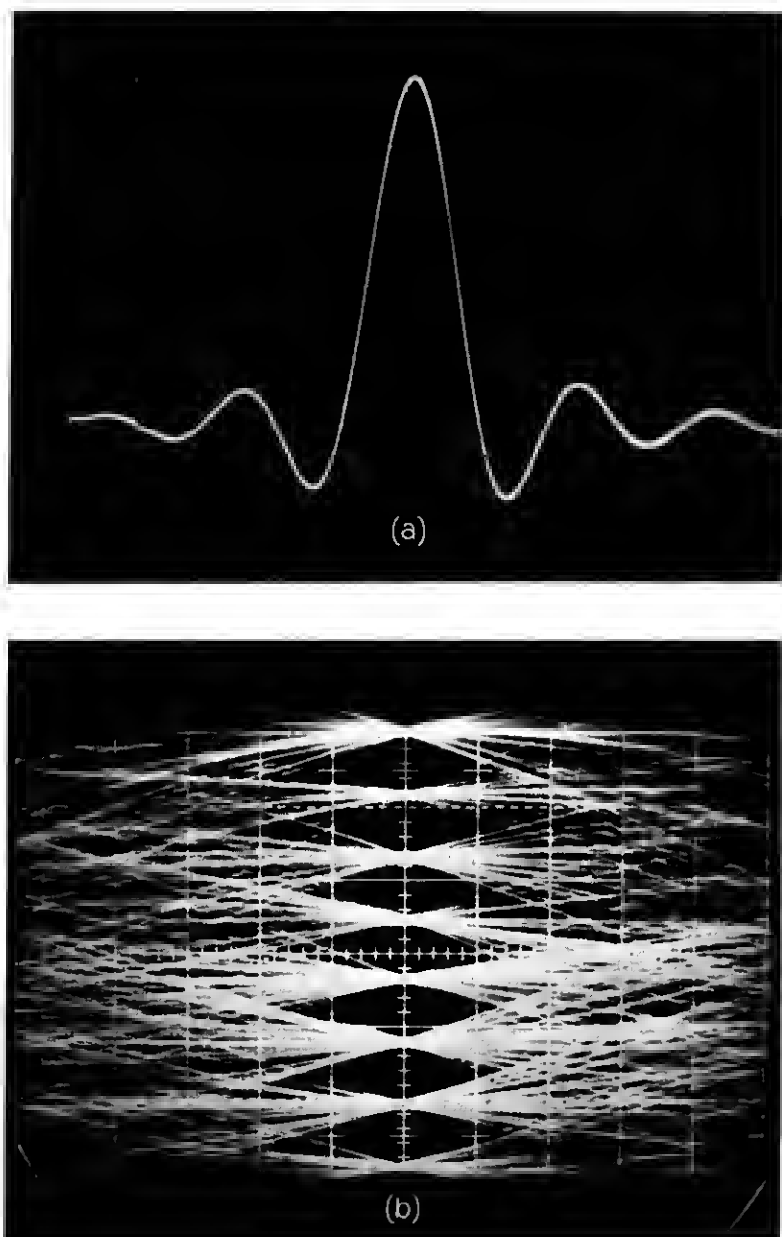


Fig. 12 — Experimental data on an active network realization of the transfer function given in Fig. 11. (a) Response of the network to a rectangular input pulse. The Nyquist frequency for the filter was 1800 Hz. (b) Eight level eye patterns generated by a random sequence of rectangular pulses with eight distinct amplitudes.

It should be stressed that although the design procedure used here gives excellent results, they are not necessarily optimum in any particular sense. It is clear from the complex way in which the poles enter into the time response of the output pulse that the error between the pulse samples, realized by equation (5) and the desired pulse samples, may not have a unique minimum; therefore, the computer program used to optimize the pole locations may actually converge to a local minimum. However, with a little experience the initial pole positions can be selected to give very satisfactory results.

IV. EXTENSIONS TO SHAPING ARBITRARY INPUTS

So far, only the shaping of a rectangular pulse has been considered. There are many situations where nonrectangular pulses must be shaped. For example, consider the case where the network is to shape a rectangular pulse to be transmitted over a channel which is no longer ideal as has been assumed so far; now the channel is assumed to introduce a known, fixed amount of amplitude and delay distortion. In this case, the pulse at the receiver is unchanged if the pulse-shaping network and the channel are interchanged (see Figs. 13a and b). Now the pulses presented to the shaping network from the channel are no longer rectangular. By having the network shape the channel output into a Nyquist pulse, the overall cascade connection of the pulse-shaping network and the channel shape a rectangular pulse into a Nyquist pulse. It is assumed that a solution to this problem is theoretically possible. A case which does not have a solution occurs when the channel is band-limited to less than $(1/2T)$ Hz.

For this example one might ask why the design process is rearranged in this manner. A more straightforward approach is to calculate the channel input required to give a particular Nyquist pulse at the channel output. The channel input is then approximated by the output of the shaping network. This approach has two disadvantages: (i) the channel output is over-specified, and (ii) the shaping network must approximate the channel input at more time points than is necessary in the other case.

In order to determine the output of the shaping network, $x(t)$, resulting from an arbitrary input, $y(t)$, one must perform a convolution. In general, a convolution is a very time-consuming calculation to carry out on a digital computer;* however, because the pulse-shaping net-

* A convolution must be performed *many* times when the poles of the pulse-shaping network are optimized by using a digital computer.

work is band-limited and we are interested in only equally spaced samples of the output pulse, this convolution can be made very efficient even without resorting to fast Fourier transform methods.

Since the pulse-shaping network is band-limited, an ideal band-limiting filter with the same bandwidth can be placed in front of it without appreciably affecting the shape of the output pulse (see Fig. 13b and c). Some effect occurs because the pulse-shaping network is not ideally band-limiting; this effect is small for reasonable stopband rejection levels. Now the input to the pulse-shaping network is band-limited. Since this is the case, the convolution can be performed using samples spaced at intervals of (π/ω_c) seconds or less, where ω_c is the cutoff frequency of the pulse-shaping network (see Figs. 13c and d). There is some aliasing error because the pulse-shaping network is not ideally band-limited; but this can be made small.

The bandwidth, ω_c , of the pulse-shaping network in all cases is greater than (π/T) radians per second (T is the time between successive pulses) and is usually less than $(2\pi/T)$ radians per second. For this situ-

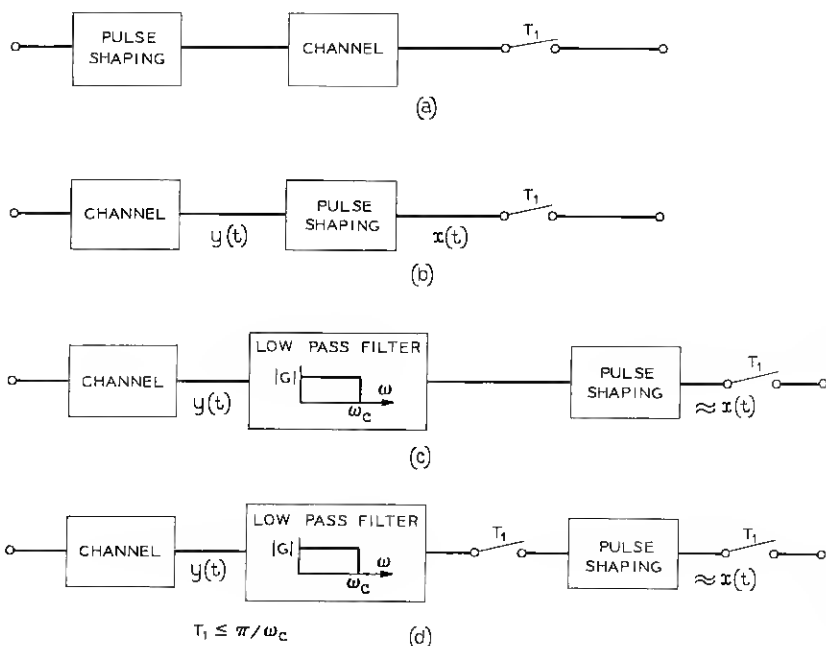


Fig. 13 — Approximately equivalent systems.

ation the output of the network can be found most conveniently by performing the convolution with samples spaced at intervals of length $T_1 = T/2$. Although a larger T_1 ($T_1 \leq \pi/\omega_c$) could be used, it requires interpolation to find the output at required sample times.

Figure 14 shows the results of the design of a pulse-shaping network to shape a nonrectangular pulse. The filters of a vestigial-sideband data transmission system were designed using a standard frequency-domain approach. The system was then simulated on a digital computer (assuming an ideal channel) and a binary eye pattern generated as Fig. 14a shows. The system was not ideal, as the figure indicates, because of errors introduced by the filters. The worst-case distortion was 64 percent.

The low-pass filter which follows the demodulator of the system was then designed, using the time-domain procedure described here. The order of the filter was kept the same. The portions of the data transmission system preceding the low-pass filter assumed the function of the channel as shown in Fig. 13. Figure 14b shows a binary eye pattern generated by a computer simulation of the data transmission system which incorporates the filter designed in the time domain. The worst-case distortion was 16 percent. The results in Fig. 14 occur without the aid of an automatic transversal equalizer.⁶ When such an equalizer is used the results for both cases improve significantly and the advantage offered by the network designed in the time domain is reduced depending, of course, on the number of taps on the equalizer.

V. CONCLUSION

This paper has discussed a method of designing networks to shape arbitrary input pulses into band-limited Nyquist pulses. A modified Temes and Gyi constraint is used to keep the shaped pulses band-limited; the time responses are then optimized only at those time instants of interest. The resulting networks accurately realize both time and frequency domain specifications with minimum network complexity.

VI. ACKNOWLEDGMENTS

The author would like to thank J. Tow and M. J. Magelnicki who designed and constructed an extremely accurate active network realization of the transfer function of Fig. 11; Figs. 7 through 12 show the characteristics of this network realization.

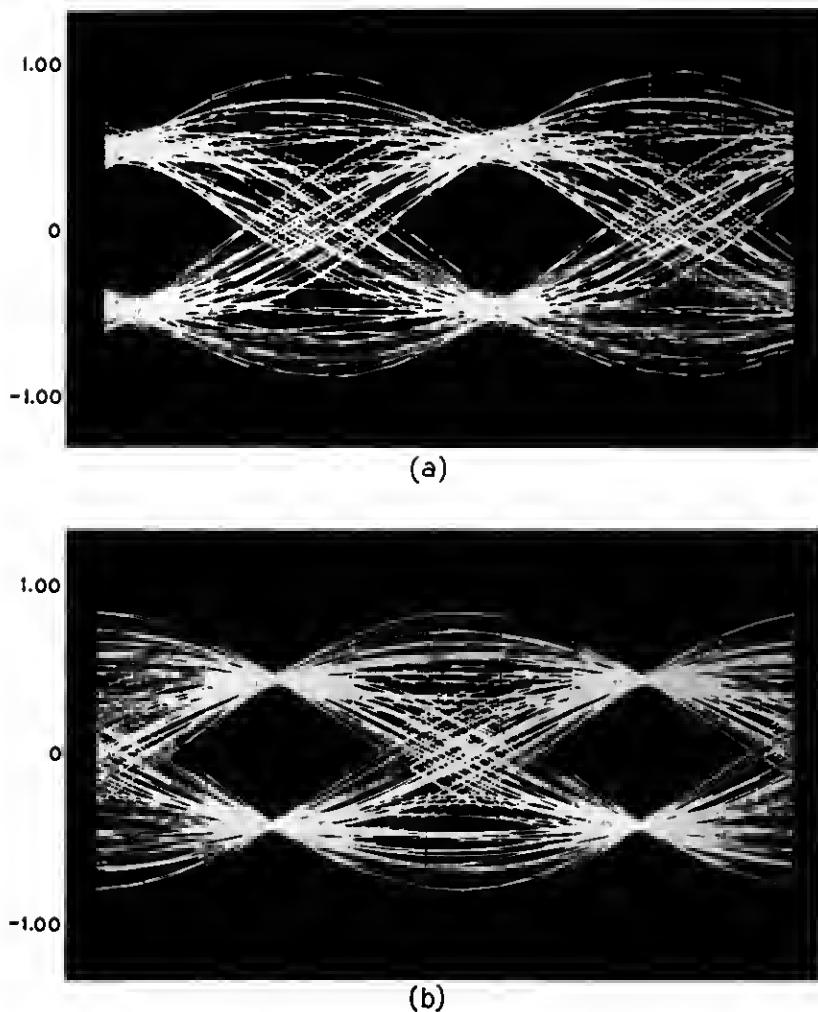


Fig. 14—Computer generated binary eye patterns for a vestigial-sideband data transmission system. (a) Results occurring when the filters are designed using frequency domain techniques. (b) Results occurring when the low-pass filter following the demodulator is designed by the technique described in Section 4.

APPENDIX

Arbitrary Passband, Equal-Ripple Stopband Transfer Function of Temes and Gyi²

This appendix explains the procedure used by Temes and Gyi to develop $G(s)$, a low-pass, equal-ripple stopband, arbitrary passband transfer function. A rational $G(s)$ should (i) realize a gain less than or equal to some constant K for frequencies in the stopband, $|\omega| \geq \omega_c$ and (ii) have an arbitrary gain in the passband, $|\omega| < \omega_c$. This is achieved basically by using the poles of $G(s)$ to give the desired passband gain and the zeros of $G(s)$ to give the desired equal-ripple stopband gain.

To develop a transfer function with the desired gain properties, we consider the function $G(s)G(-s)$. For $s = j\omega$, $G(s)G(-s)$ equals the magnitude squared of $G(j\omega)$. Now consider the mapping of equation (6) which maps the s -plane to the z -plane:

$$z^2 = s^2 + \omega_c^2, \quad \operatorname{Re}(z) \geq 0, \quad z = x + jy. \quad (6)$$

This mapping causes the stopband portion of $j\omega$ axis in the s -plane to correspond to the entire jy axis of the z -plane and the passband portion of the $j\omega$ axis in the s -plane to correspond to a portion of the x axis of the z -plane. The function $G(s)G(-s)$ can be transformed by equation (6) to the z -plane and, as will be shown, can be made to have equal-ripple stopband behavior by giving it the form of $H(z)$ in equation (7), where

$$H(z) = \frac{K^2}{1 + R(z)R(-z)} \quad (7a)$$

and

$$R(z) = zF(z)/E(z). \quad (7b)$$

$R(z)$ is a z -plane reactance function, and $E(z)$ and $F(z)$ are even functions. By transforming $H(z)$ to the s -plane and properly factoring it into $G(s)G(-s)$, the equal-ripple stopband transfer function is generated.

The z -plane reactance function in equation (7b) is written as an odd function over an even function. The reactance function could be the reciprocal of equation (7b); but, this form would not yield a rational $G(s)$. Since a reactance function has alternating poles and zeros on the jy axis and is pure imaginary there, $H(jy)$ has equal-ripple behavior ranging between K^2 when jy is a zero of $R(z)$ and zero when jy is a pole of $R(z)$. If $F(z)$ and $E(z)$ are the same order, $R(z)$ has a

pole at infinity; therefore, $G(s)$ has a zero at infinity. If $F(z)$ is of order two less than $E(z)$, $R(z)$ has a zero at infinity and $G(s)$ is not zero at infinity.

To determine $G(s)$ explicitly, $H(z)$ is transformed into the s -plane and factored. To do this, $H(z)$ is written, using equation (7), as

$$H(z) = \frac{K^2 E^2(z)}{E^2(z) - z^2 F^2(z)} = \frac{K^2 E^2(z)}{[E(z) - zF(z)][E(z) + zF(z)]}. \quad (8)$$

Since $zF(z)/E(z)$ is a reactance function, $E(z) + zF(z)$ has roots in the left-half z -plane and $E(z) - zF(z)$ has roots in the right-half z -plane. Assuming that the polynomial $E(z) + zF(z)$ is n th order and the coefficient of z^n is unity, equation (8) can be factored into

$$H(z) = \frac{K^2 E^2(z)}{\left[\prod_{i=1}^n (z_i - z) \right] \left[\prod_{i=1}^n (z_i + z) \right]} = \frac{K^2 E^2(z)}{\prod_{i=1}^n [z_i^2 - z^2]}$$

where z_i are the roots of $E(z) - zF(z) = 0$. Using equation (6) and $s_i^2 = z_i^2 - \omega_c^2$, the s -plane version of $H(z)$ becomes

$$H(s) = \frac{K^2 E^2(z) \big|_{z^2 = s^2 + \omega_c^2}}{\prod_{i=1}^n (s_i^2 - s^2)} = \left[\frac{KE(z) \big|_{z^2 = s^2 + \omega_c^2}}{\prod_{i=1}^n (s - s_i)} \right] \left[\frac{KE(z) \big|_{z^2 = s^2 + \omega_c^2}}{\prod_{i=1}^n (-s - s_i)} \right] \\ = G(s)G(-s).$$

The s_i are the left-half plane images of the z_i . Therefore,

$$G(s) = \frac{KE(z) \big|_{z^2 = s^2 + \omega_c^2}}{\prod_{i=1}^n (s - s_i)} \quad (9)$$

is a realizable, rational transfer function. Note that $E(z)$ is an even function of z and thus is a rational function of s . Also all the zeros of $G(s)$ lie on the $j\omega$ axis in the stopband.

The construction of $G(s)$ is such that the poles, s_i , can be arbitrary (of course constrained to occur in complex conjugate pairs in the left-half plane). The numerator of $G(s)$ is found as a function of the poles by computing the polynomial

$$E(z) - zF(z) = \prod_{i=1}^n (z_i - z),$$

where $z_i^2 = s_i^2 + 1$, $\text{Re}(z_i) > 0$. The even part is taken and transformed back to the s -plane.

$G(s)$ can conveniently be expressed in partial fraction form as

$$G(s) = \sum_{i=1}^n \frac{R_i}{s - s_i}, \quad (10a)$$

$$R_i = \frac{KE(z_i)}{\prod_{\substack{k=1 \\ k \neq i}}^n (s_i - s_k)}, \quad (10b)$$

where all the poles are assumed to be distinct and n is odd, so that $G(s)$ has a zero at infinity. $E(z_i)$ can be simplified:

$$E(z) + zF(z) = \prod_{k=1}^n (z_k + z),$$

$$E(z_i) + z_i F(z_i) = 2z_i \prod_{\substack{k=1 \\ k \neq i}}^n (z_k + z_i),$$

and

$$E(-z_i) - z_i F(-z_i) = 0 = E(z_i) - z_i F(z_i).$$

The last equation is true since $E(z)$ and $F(z)$ are even functions of z . Adding the last two equations gives

$$E(z_i) = z_i \prod_{\substack{k=1 \\ k \neq i}}^n (z_k + z_i),$$

which results in

$$R_i = Kz_i \prod_{\substack{k=1 \\ k \neq i}}^n \frac{z_i + z_k}{s_i - s_k}. \quad (10c)$$

Thus, if the poles s_i are given, the residues R_i found from equation (10c) give a transfer function with equal-ripple stopband behavior.

Using this result the impulse response of $G(s)$ becomes, for odd n ,

$$g(t) = R_n \exp(s_n t) + \sum_{i=1}^{\frac{n-1}{2}} \exp[\operatorname{Re}(s_i)t] \cdot [2 \operatorname{Re}(R_i) \cos\{\operatorname{Im}(s_i)t\} - 2 \operatorname{Im}(R_i) \sin\{\operatorname{Im}(s_i)t\}]. \quad (11)$$

The real pole is s_n .

REFERENCES

1. Lucky, R. W., Salz, J., and Weldon, E. J., *Principles of Data Communication*, New York: McGraw-Hill, 1968, Chapter 4.
2. Temes, G. C., and Gyi, M., "Design of Filters with Arbitrary Passband and Chebyshev Stopband Attenuation," 1967 IEEE Int. Conv. Digest, March 20-23, 1967, Paper 23.1, pp. 184-185.
3. Ulstad, M. S., "Time Domain Approximations and An Active Network Realization of Transfer Functions Derived From Ideal Filters," IEEE Trans. Circuit Theory, *CT-15*, No. 3 (September 1968), pp. 205-210.
4. Jess, J., and Schüssler, H. W., "On the Design of Pulse-Forming Networks," IEEE Trans. Circuit Theory, *CT-13*, No. 3 (September 1965), pp. 393-400.
5. Tow, J., "Active RC Filters—A State-Space Approach," Proc. IEEE, *56*, No. 6 (June 1968), pp. 1137-1139.
6. Lucky, R. W., "Techniques for Adaptive Equalization of Digital Communication," B.S.T.J., *45*, No. 2 (February 1966), pp. 255-286.